

Schuler Tuned Vertical Indicating System

S. J. Monaco* and D. R. Audley†
U. S. Air Force Academy, Colo.

and

S. Okubo‡
Okubo Instruments, Colorado Springs, Colo.

A single-axis, gyroless, vertical indicating system which tracks the motion of the local gravity vector has been designed and built. This system was developed in a research program to demonstrate the feasibility of using it in a low-cost, high-reliability, medium-accuracy navigator. This system is capable of sensing accelerations as small as $10^{-4}g$ and uses only a compound pendulum and a rotor as its sensing elements, both made with fused quartz suspensions. Input linear accelerations normally causing the pendulum to rotate are sensed by the rotor, and proportional signals are fed back to a torquing system to maintain the pendulum's vertical reference. An output signal proportional to the tangential acceleration is also provided. This paper addresses only the questions of concept and design and discusses preliminary test results on a research model. Although the technical concept considered the objectives of low-cost and medium-accuracy, no attempt has been made to address these issues, as they would pertain to an actual navigation system, at this time. Two research models of this device were built and tested. The total cost of parts, including electronics, for these models was under \$600.

Introduction

PRECISE knowledge of the Earth's gravitational field provides an extremely accurate and simple reference for navigation. Although there are several schemes for determining the direction of the local vertical, by far the most accurate is a "Schuler tuned" vertical indicating system. Such a classical approach to tracking the local vertical vector has been developed using rate gyros.¹⁻³ An example of this is the Rate and Acceleration Measuring Pendulum (RAMP) built by the Swedish Philips Co. Ltd. This system used only three gyros of relatively low quality to obtain a local vertical navigator with high accuracy. Subsequent work by Koenke⁴ followed, which had as its objective an explanation of how the high navigational accuracy was obtained with these relatively crude sensors (fire control gyros). His conclusion was that the error mechanisms for the RAMP were identical to those of a conventional system for identical sources; however, the additional isolation provided to the gyros resulted in better gyro performance.

Although the performance of the RAMP was quite good, it was never adopted for use in a major avionics system. Perhaps one of the reasons for this is that it still required the use of gyros—inherently noisy instruments since they require high-speed rotors and relatively high power consumption. The vertical indicating system presented in this article eliminates the use of a gyro, replacing it with an angular differentiating accelerometer. Thus, this system has been termed an angular accelerometer stabilized pendulum (AASP). However, unlike the RAMP, which used an azimuth gyro for azimuth navigation, a navigator mechanized with the AASP will require an additional angular accelerometer with its sensitive axis aligned with the vertical axis.

The elimination of the gyroscope is also proposed in order to improve the system reliability and reduce the costs while maintaining similar performance standards. The AASP was designed to meet the requirements for a high-reliability, low-cost, medium-accuracy navigator. Specifically, the total system navigation error was to be less than 1 nm/h and the total system cost less than \$5000. The reliability was addressed by eliminating high-speed moving parts, pressurized bearings, and high power requirements. In fact, part of the design philosophy was to build a model out of common stock items such as aluminum and plexiglass without the need for critical tolerances or sophisticated assembly techniques. The verification of whether or not the AASP did or will ever meet the accuracy and cost requirements is not within the scope of this work.

The utilization of an angular motion sensor (AMS) made the implementation of this sensor straightforward. Exotic or complex techniques were not required. This system is rather a direct offshoot of the floated gyro/accelerometer technology to an even simpler, more direct mechanization, which eliminates most of the complexity of existing sensors.

The objective of this system is to eliminate the sensitivity of a pendulum to horizontal accelerations at the point of suspension (pivot point). A mechanization of this would be a simple physical pendulum with length equal to the radius of the Earth, which has a period of 84.4 min. Alternatively, if the moment of inertia of the pendulum about its pivot is simulated using acceleration feedback, the pendulum may be made insensitive to pivot accelerations and, therefore, track the local gravity vector. In this resulting electromechanical system, the pendulum will be insensitive to tangential accelerations and hence we will refer to it as "Schuler tuned."

Referring to Fig. 1, the angular accelerometer mounted integrally with the pendulum responds to the rotation of the pendulum (θ_p) caused by the horizontal accelerations of the sensor case. The output of the accelerometer is fed back through a servo to the pendulum torquer and keeps the pendulum vertical. Since $\ddot{\theta}_p = a/\rho$ (where ρ = length of pendulum), the integral of the θ_p signal is proportional to the linear velocity of the sensor case. This derived rate may be used to provide inputs to a navigation computer.

The isolation gimbal is slaved to the pendulum by the gimbal torquer. Thus, an angular position pickoff located on the gimbal axis reads out directly the Euler angle of the sensor

Presented as Paper 77-1066 at the AIAA Guidance and Control Conference, Hollywood, Fla., Aug. 8-10, 1977; submitted Sept. 9, 1977; revision received April 27, 1978. Copyright © American Institute of Aeronautics and Astronautics, Inc., 1977. All rights reserved.

Index categories: Navigation, Communication, and Traffic Control; Guidance and Control.

*Research Associate, Frank J. Seiler Research Laboratory. Member AIAA.

†Research Associate, Frank J. Seiler Research Laboratory.

‡President. Member AIAA.

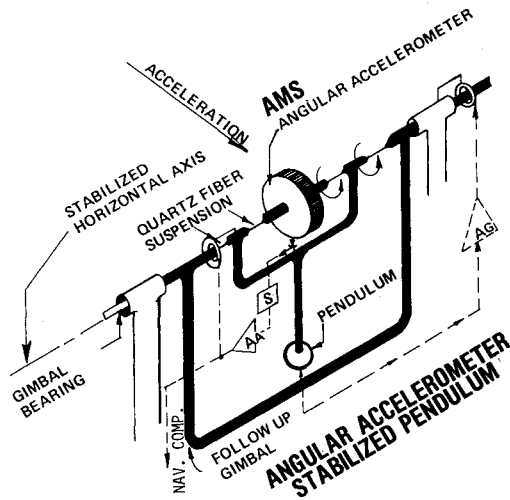


Fig. 1 A gyroless vertical indicating system.

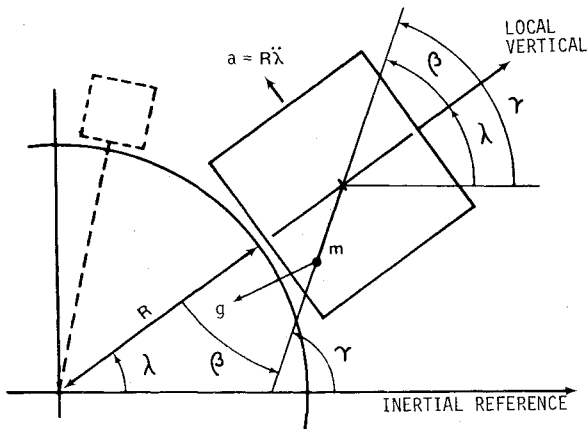


Fig. 2 Motion of a simple pendulum.

body-mounted coordinate system. This would correspond to the roll or pitch angle as illustrated on the figure. There is very little error torque disturbance that can be transmitted to the pendulum due to the isolation gimbal. The only significant error sources would be the friction on the gimbal axis bearings.

The critical bearings are the angular accelerometer and pendulum axis suspensions. The AASP utilizes a fused quartz fiber suspension that is virtually error free. Both the angular accelerometer and the pendulum are made neutrally buoyant in a medium density fluid to enhance the environmental capability of these suspensions. This ensures a high g capability.

Analytical Development

Motion of a Simple Pendulum Due to Tangential Acceleration

In developing the equations of motion for the AASP, it is perhaps helpful to consider first the special case of Schuler tuning a simple pendulum of length ℓ and bob mass m . In Fig. 2, λ refers to the angle of local vertical with respect to an inertial reference; β refers to the angle of the pendulum with respect to the local vertical; γ , the angle of the pendulum with respect to an inertial reference; and R is the Earth radius.

The motion of the system is then described by equating the rate of change of angular momentum $H(t)$ to the sum of the moments $M_i(t)$ about the pivot point:

$$\frac{d}{dt} H(t) = \sum_{i=1}^n M_i(t) \quad (1)$$

For this simple case with tangential acceleration $a(t)$ and small displacement (β):

$$I\ddot{\beta}(t) + I\ddot{\lambda}(t) = -m\ell g\beta(t) + m\ell a(t) \quad (2)$$

where $I = m\ell^2$ (inertia term), $m\ell g\beta$ is the restoring moment due to gravity, and $m\ell a$ the moment due to tangential acceleration.

Equivalently, in inertial coordinates (let $\gamma = \beta + \lambda$), and letting $a = R\lambda$, we have

$$I\ddot{\gamma}(t) = -m\ell g[\gamma(t) - \lambda(t)] + m\ell R\ddot{\lambda}(t) \quad (3a)$$

or

$$I\ddot{\gamma}(t) + m\ell g\gamma(t) = m\ell R\ddot{\lambda}(t) + m\ell g\lambda(t) \quad (3b)$$

When $\gamma(t) = \lambda(t)$ the pendulum will "track" the local vertical and is insensitive to tangential accelerations. This is the condition of Schuler tuning. A physical mechanization of this condition is to let $\ell = R$ (Earth radius). Then, since $I = m\ell^2$, Eq. (3) becomes

$$\ddot{\gamma}(t) + (g/R)\gamma(t) = \ddot{\lambda}(t) + (g/R)\lambda(t) \quad (4)$$

$\gamma(t) = \lambda(t)$, and the period of this system is the usual 84.4 min. Since $\ell = R$ is physically unrealizable, electromechanical realizations of this system have been suggested.

Let $T_p = -K\ddot{\gamma}(t)$ represent a feedback torque at the pivot point proportional to $\ddot{\gamma}(t)$. Then Eq. (3) becomes

$$(I+K)\ddot{\gamma}(t) + m\ell g\gamma(t) = m\ell R\ddot{\lambda}(t) + m\ell g\lambda(t) \quad (5)$$

and, when $K = m\ell R - I$, we obtain

$$\ddot{\gamma}(t) + (g/R)\gamma(t) = \ddot{\lambda}(t) + (g/R)\lambda(t)$$

which is readily recognized as satisfying the Schuler tuned condition.

Motion of a Compound Pendulum Due to Tangential Acceleration

In the same manner, the motion of a compound pendulum due to tangential accelerations may be derived. The compound pendulum, depicted in Fig. 3, has both viscous damping and a torsional spring force associated with it. The equation of motion in inertial coordinates is

$$I\ddot{\gamma}(t) + b_p\dot{\gamma}(t) + (k_p + m\ell g)\gamma(t) = m\ell R\ddot{\lambda}(t) + b_p\dot{\lambda}(t) + (k_p + m\ell g)\lambda(t) \quad (6)$$

where b_p is the damping coefficient and k_p the torsional spring rate.

The hypothesized feedback torque for Schuler tuning is again $T_p = -K\ddot{\gamma}(t)$, and provides the equation:

$$(I+K)\ddot{\gamma}(t) + b_p\dot{\gamma}(t) + (k_p + m\ell g)\gamma(t) = m\ell R\ddot{\lambda}(t) + b_p\dot{\lambda}(t) + (k_p + m\ell g)\lambda(t) \quad (7)$$

This system also satisfies the Schuler tuned condition when $K = m\ell R - I$. This is depicted in block diagram form in Fig. 4.

Measuring Angular Acceleration

An angular motion sensor (AMS) was chosen to measure $\dot{\gamma}(t)$. This device is essentially a symmetric disk with a quartz fiber suspension system and a velocity (moving coil) pickoff. That is, the output voltage V_o is proportional to an input velocity $\dot{\theta}$. This velocity pickoff has a characteristic response function that is flat to inputs of $\dot{\gamma}$; i.e., the derivative of acceleration, below its natural frequency.⁵ This is depicted in Fig. 5. Because of its characteristic frequency response, this particular angular motion sensor may be described as an

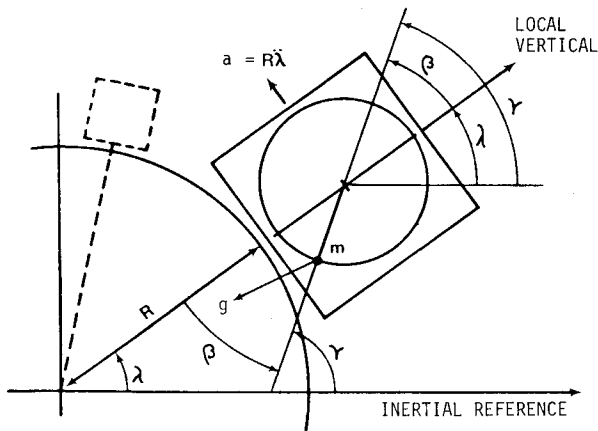


Fig. 3 Motion of a compound pendulum.

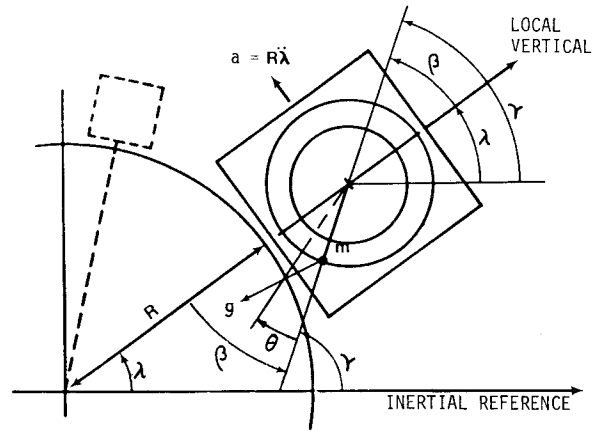


Fig. 7 Dynamics of the angular accelerometer Schuler pendulum.

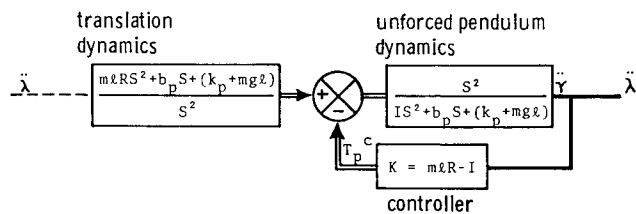


Fig. 4 Block diagram of Schuler tuned compound pendulum (note: $\ddot{\gamma} = \ddot{\lambda}$ when $K = mlR - I$).

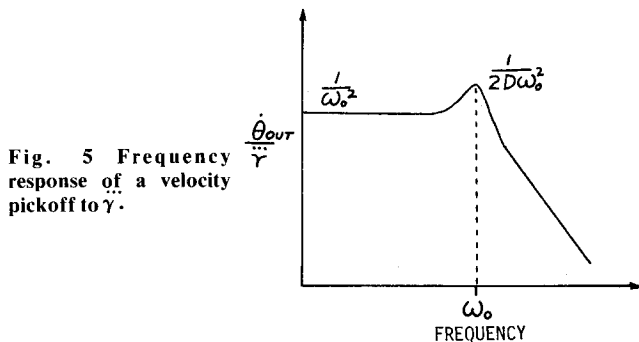


Fig. 5 Frequency response of a velocity pickoff to $\dot{\gamma}$.

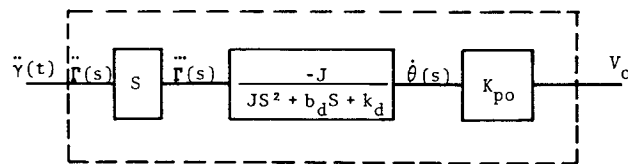


Fig. 6 Block diagram of angular motion sensor.

“angular differentiating accelerometer.” The motion of the inertial disk to a reference input may be described by $J\ddot{\gamma}(t) + J\ddot{\theta}(t) = -b_d\dot{\theta}(t) - k_d\theta(t)$, and the mathematical model relating the output voltage V_o to the acceleration input, $\ddot{\gamma}(t)$, is given by

$$-J \frac{d}{dt} \ddot{\gamma}(t) = \frac{J}{K_{po}} \ddot{V}_o(t) + \frac{b_d}{K_{po}} \dot{V}_o(t) + \frac{k_d}{K_{po}} V_o(t) \quad (8)$$

where J is the inertia of the disk, k_d the torsional spring constant, b_d the damping coefficient, and K_{po} the pickoff scale factor.

The block diagram for this sensor is shown in Fig. 6. The transfer function is then represented by

$$\frac{\dot{\theta}(s)}{\ddot{\Gamma}(s)} = \frac{-J/k_d}{(J/k_d)s^2 + (b_d/k_d)s + I}$$

and we note that for inputs (angular motions) with frequency $\omega < \omega_{nd} = \sqrt{k_d/J}$, this is well represented by

$$\frac{\dot{\theta}(s)}{\ddot{\Gamma}(s)} = -\frac{J}{k_d} = -\frac{I}{\omega_{nd}^2} \quad (9)$$

Angular Accelerometer Schuler Pendulum

The AASP is the composite of the compound pendulum and the AMS previously described. This system is depicted in Fig. 7. Noting the coupling terms $k_d\theta(t)$ and $b_d\dot{\theta}(t)$ between the disk and pendulum and incorporating these into Eq. 6 yields the pendulum equation:

$$I\ddot{\gamma}(t) + b_p\dot{\gamma}(t) + (k_p + mgl)\gamma(t) = mlR\ddot{\lambda}(t) + b_p\dot{\lambda}(t) + (k_p + mgl)\lambda(t) + b_d\dot{\theta}(t) + k_d\theta(t) + T_p \quad (10)$$

Also recall that for $\omega < \omega_{nd} = \sqrt{k_d/J}$, the AMS is represented by $k_d\theta(t) = -J\ddot{\gamma}(t)$ and, equivalently, $k_d\dot{\theta}(t) = -J\dot{\gamma}(t)$. Substituting these relations into Eq. (10) yields

$$(b_d/k_d)J\dot{\gamma}(t) + (I+J)\ddot{\gamma}(t) + (b_p\dot{\gamma}(t) + (k_p + mgl)\gamma(t)) = mlR\ddot{\lambda}(t) + b_p\dot{\lambda}(t) + (k_p + mgl)\lambda(t) + T_p \quad (11)$$

which describes the motion of the AASP for $\omega < \omega_{nd}$.

Schuler Tuning

To satisfy the Schuler tuning condition, we find that

$$T_p = -K_1\dot{\gamma}(t) - K_2\ddot{\gamma}(t)$$

where

$$K_1 = -(b_d J/k_d) = K_T K_V \quad (12)$$

$$K_2 = mlR - I - J = K_T K_P \quad (13)$$

when $\omega < \omega_{nd}$. These represent the theoretical “Schuler gains” that must be obtained. This system is depicted in block diagram form in Fig. 8. In this diagram we have defined the parameters:

$$\omega_{np} = \sqrt{\frac{k_p + mgl}{I}} \quad \omega_{nd} = \sqrt{\frac{k_d}{J}} \quad \zeta_p = \frac{b_d}{2\sqrt{I(k_p + mgl)}} \quad \zeta_d = \frac{b_d}{2\sqrt{k_d J}}$$

Incorporating the simplified AMS model [Eq. (9)] into this yields the reduced block diagram shown in Fig. 9.

Model Verification

Both open-loop and closed-loop responses, as obtained from the preceding analysis, were simulated on a PDP 11/45 computer. Then data were taken in the frequency range of 0.8

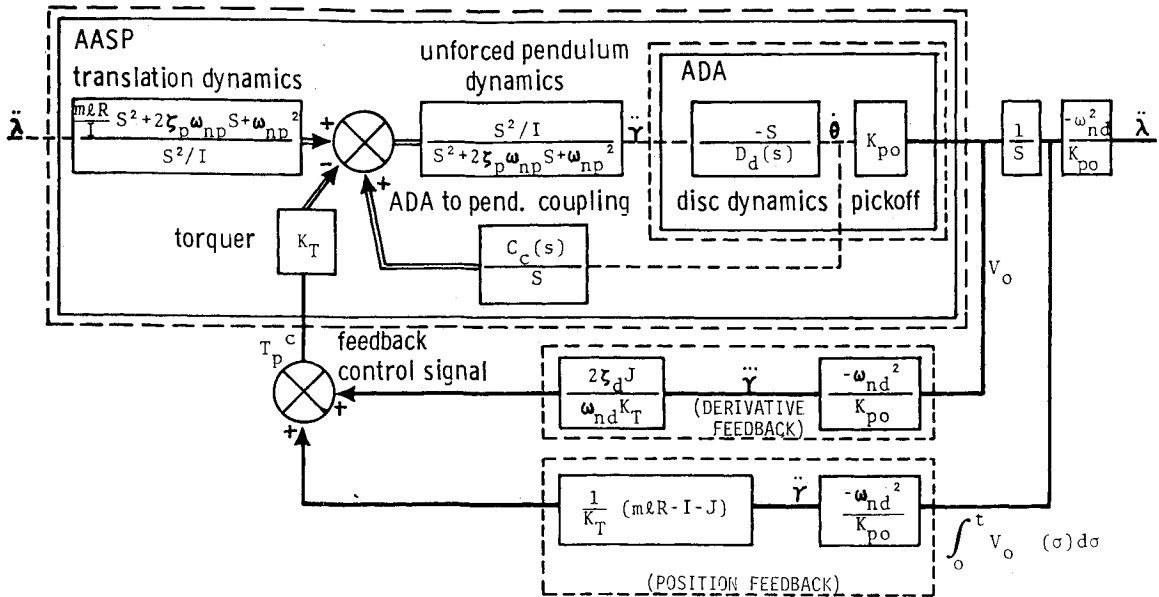


Fig. 8 Block diagram of AASP.

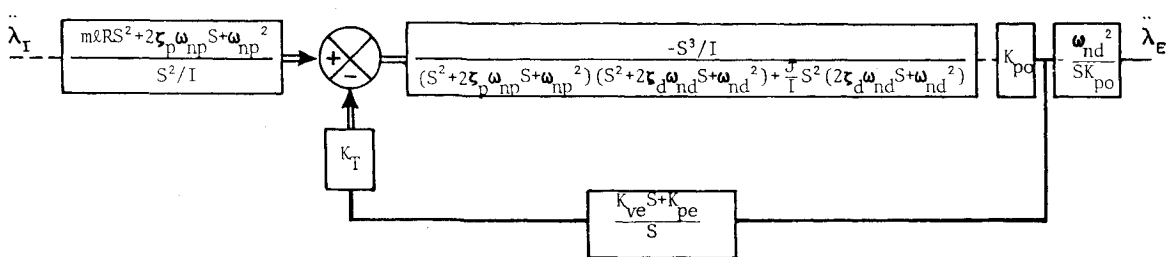


Fig. 9 Equivalent "reduced" block diagram.

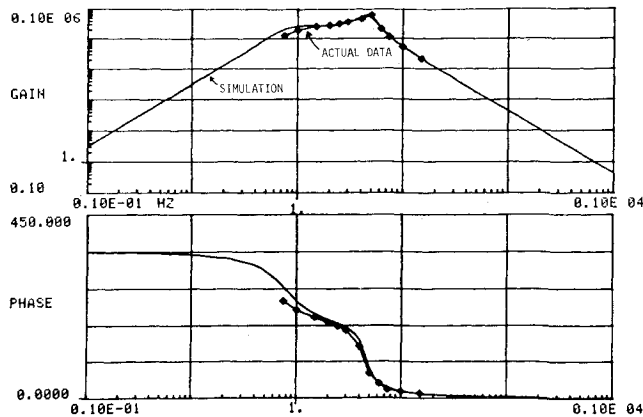


Fig. 10 Actual and simulated open-loop response.

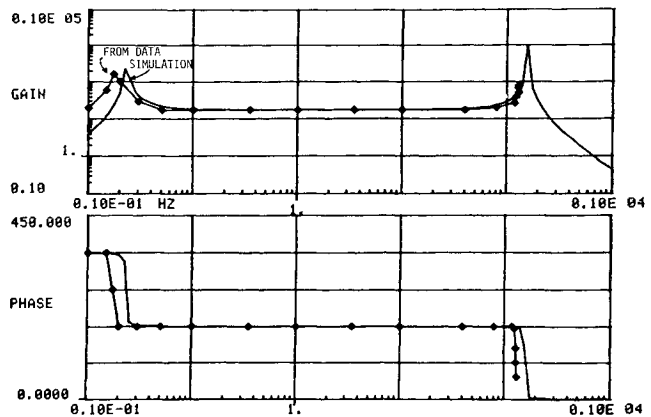


Fig. 11 Actual and simulated closed-loop response.

Hz to 20 Hz. These simulated and actual transfer functions are compared in Figs. 10 and 11. The complete description of how these data were collected is given in a later section.

Mechanical Design

The mechanical design of the AASP can be described in terms of the transfer function obtained from the mathematical model of Fig. 9. The performance of the AASP is determined by the location of the undamped natural frequencies of the pendulum ω_{np} and the accelerometer ω_{nd} . They are hollow cylinders made neutrally buoyant in the flotation fluid. Both cylinders are symmetrical designs so that the center of buoyancy and the center of suspension are coincident. Twelve pairs of samarium cobalt magnets are mounted on the pendulum. Three pairs of these magnets interact with the three pickoff coils that are mounted on the

accelerometer. The alternate remaining pairs of magnets interact with the three torquer coils mounted on the case shown in Fig. 12. After the balancing procedure, a known pendulosity, $mg\ell$, is added to the pendulum.

The pendulum and accelerometer are suspended on pairs of fused quartz filaments shown in Fig. 13. The colinear design of these suspensions makes a one-piece design possible. The quartz suspension features a low coefficient of thermal expansion (0.5×10^{-6} cm/cm), very low mechanical hysteresis and high tensile strength. The joints are all fused to the quartz frame, which separates the pendulum from the accelerometer. In this subassembly the undamped natural frequencies are checked.

The pendulum/accelerometer assembly is then enclosed in the case (see Fig. 13). Once assembled and sealed, one end of the quartz filament is cemented in place. The other end has :

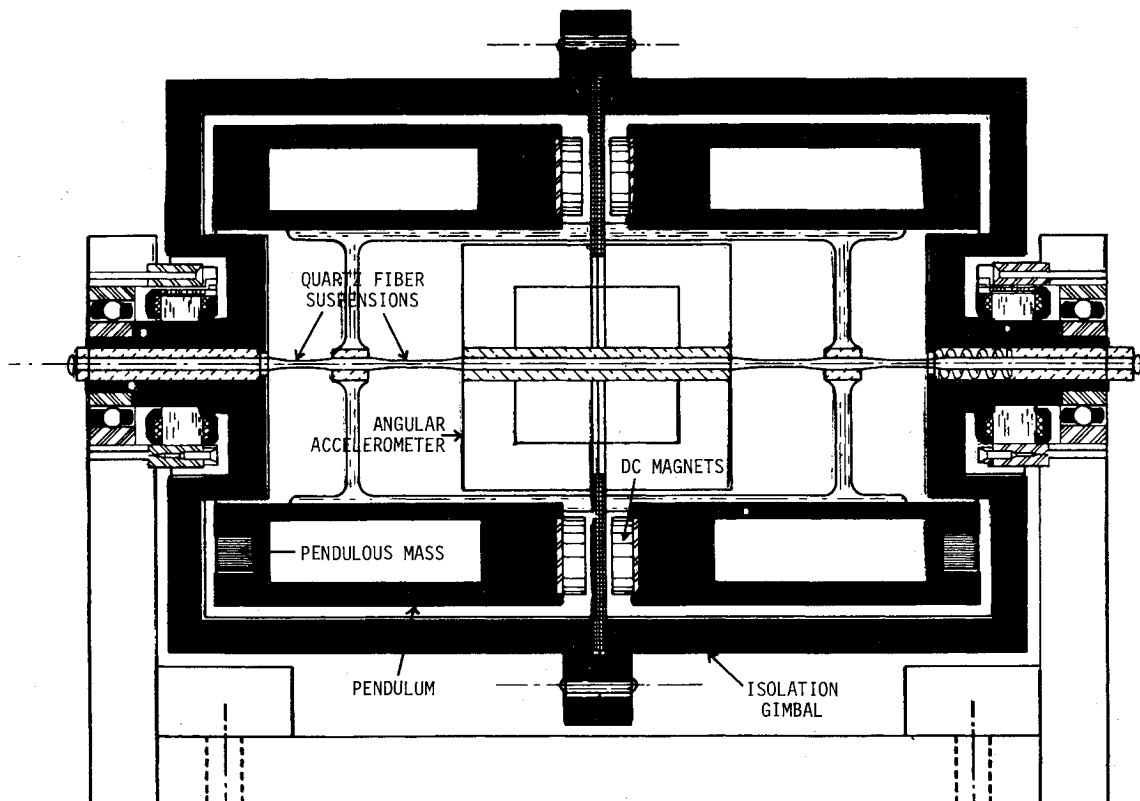


Fig. 12 Cross-sectional view of angular accelerometer Schuler pendulum.

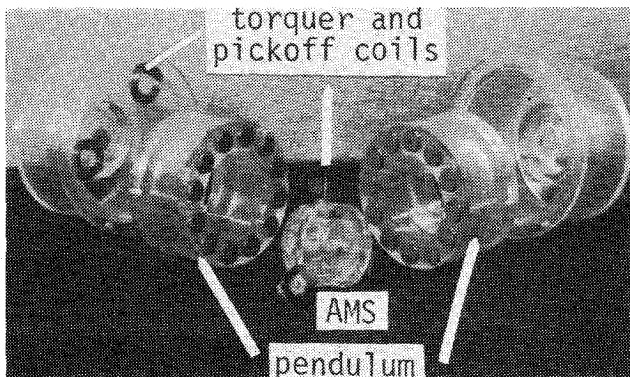


Fig. 13 AASP subassemblies.

1-kg preloading spring mechanism to accommodate the differential thermal expansion between the case and the quartz frame assembly. The flotation fluid is common to both assemblies and controls the damping (ζ) of the sensors. The fluid is Dow 200 silicone.

The AASP is then mounted in a frame assembly with ball bearings. This arrangement can be looked upon as an isolation gimbal. A pickoff between the pendulum and the case is used to keep the case slaved to the pendulum independently of the orientation of the frame assembly. For this purpose a torquer is required between the frame and the case. A resolver is located on the other end, and it can be used to read out the Euler angles.

In the prototype the size of the model depended primarily on the specific gravity of the flotation fluid, which is nearly equal to that of water. By utilizing higher density fluids, the size can be readily reduced by a factor of 3. The weight of the magnet assembly also determines the size of the pendulum float. The actual magnets used were off-the-shelf units. By incorporating a special design, smaller assemblies are possible.

The prototype shows the elegant simplicity of the AASP concept that replaces a gyroscope and linear accelerometer in conventional systems. No power is required and therefore no "active" elements are required. When higher-density fluids are used, heaters will be required.

In the course of this program, the AASP had to be disassembled many times. Even though it is built of plastic, no part had to be rebuilt, except for the quartz fiber assembly. The turn-around time was reduced to two days by the end of the project. The final design calls for an all fused quartz assembly (with exception of magnets and coils).

Testing

This section describes the tests that were performed on a research model of the AASP in order to verify the performance model and to determine some basic sensitivities. Since the AASP is a stabilized platform that will measure accelerations tangential to the locally maintained vertical reference, an application of linear acceleration along its sensitive axis is the most desirable test environment. However, linear shaker tables capable of up to 5-g inputs at frequencies from 0.01 Hz to 10 Hz were not available. Therefore, a technique which involved direct excitation of the pendulum torquer was employed. In this test configuration the torquer was excited either with discrete frequencies or white noise in a particular frequency band. This test provided both open-loop and closed-loop responses depending on a switch in the torquing loop being open or closed. The only part of the system bypassed in these tests was the AASP translation dynamics (see Fig. 8). The electronics configuration for these tests is shown in Fig. 14.

The test results demonstrated the critical importance of achieving the proper gain in both the position and derivative feedback loops. A flat frequency response to an input voltage at the torquer (acceleration input) and a velocity output is obtained only when these gains are optimized. The proportion of derivative gain to position gain is also critical. By careful

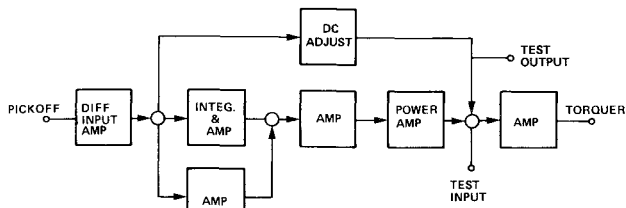


Fig. 14 AASP electronics test configuration.

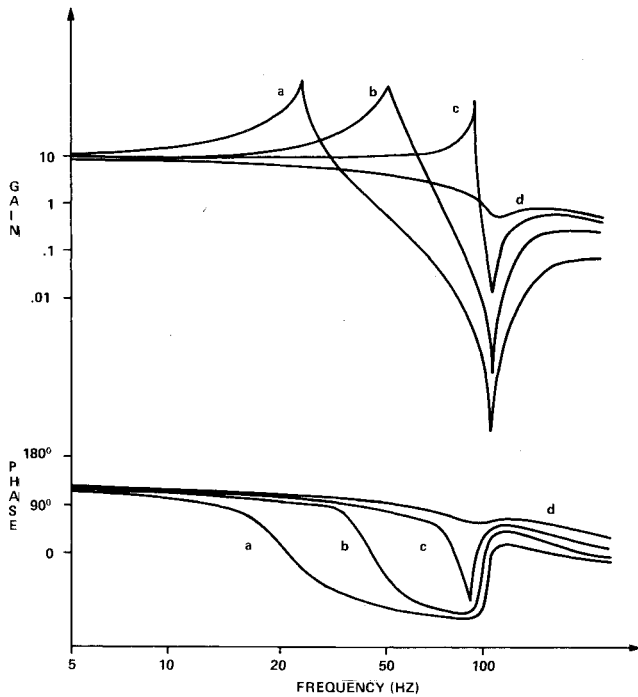


Fig. 15 Effect of increasing position feedback gain (a to d).

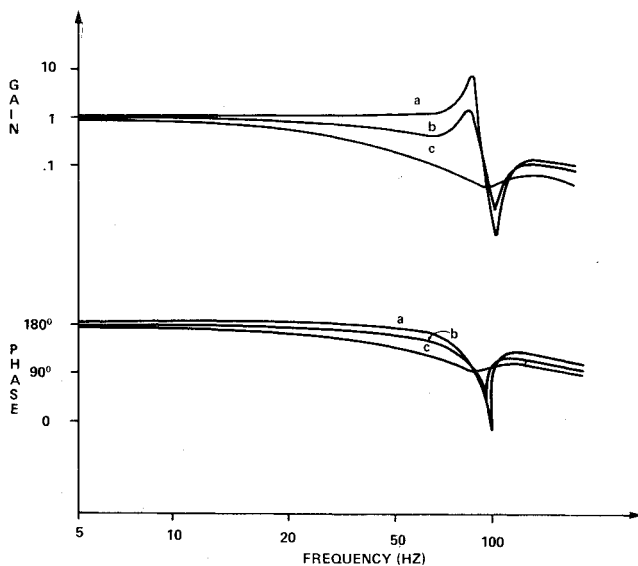


Fig. 16 Effect of increasing velocity (derivative) feedback gain (a to c).

“tuning”, i.e., selection of the proper gains for both the position and derivative feedbacks, the desired response characteristics were obtained. The effect of increasing the position and derivative feedbacks is shown in Figs. 15 and 16, respectively. The gain in the former was increased from 2×10^5 to 5×10^7 (a to d), and decreased from 200 to 100 (a to c) in the latter. Note that a smaller percentage change in the

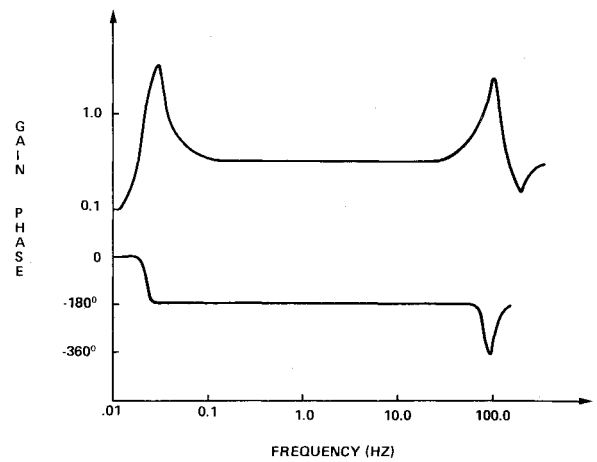


Fig. 17 AASP closed-loop response with “optimized” gains.

velocity feedback is needed to produce approximately the same magnitude change in the closed-loop response. Although the velocity feedback gain is small in relation to the position feedback gain, it is extremely important and cannot be eliminated. This former loop gain may be interpreted as an “anticipative” signal to which the system response is extremely sensitive.

Optimizing both feedback gains yields the desirable flat operating region. If the theoretical “Schuler gains” are obtained (see Eqs. 12 and 13), then the response would be completely flat from the “Schuler frequency” on up. However, it is really not necessary to achieve this type of response for most applications. For example, using gains achieved on breadboarded electronics of 10^7 and 10^3 for the position and velocity feedbacks, respectively, achieves the results shown in Fig. 17. Here we have obtained a flat region from approximately 0.03 Hz to 60 Hz. This would be sufficient for most guidance applications.

In addition to these tests demonstrating the overall AASP response characteristics, scale factor linearity and threshold sensitivity tests were run. The scale factor obtained with the first prototype was 4.0 V/g. Threshold tests showed a clear sensitivity to inputs as small as $10^{-4}g$ corresponding to an output signal of 0.4 mV. A scale factor linearity test run between $10^{-4}g$ and 1 g showed less than 4% deviation in scale factor over this range.

Summary

Design

The AASP is based upon the concept of Schuler tuning a vertical pendulum in order to desensitize it to accelerations tangential to the local vertical. Although this has been demonstrated before in the RAMP system, the novelty of this approach has been to eliminate the use of gyros, thus removing the major error source in such a system. There are neither drift errors nor bias and null uncertainties in the AASP. In addition, it is inherently self-correcting in the sense that the pendulum is stable under steady-state velocities and torquing is required only during periods of acceleration. Although the use of a velocity pickoff requires an added integration step, the effect of integration errors is minimized, since it is used outside the control loop. On the other hand, no power is required for velocity pickoff, and thus no reaction torques, null shifts, or thermal instabilities are generated. The quartz fiber suspension used for both the pendulum and angular accelerometer are ideal for a null-type instrument since there is no measurable bearing friction or hysteresis. The complete symmetry of the design on coaxial suspensions minimizes cross coupling effects. Anisoeasticity is also eliminated by making all the critical subcomponents neutrally buoyant.

Performance

Although the tests that have been described had as their objective only a demonstration of feasibility, we feel that they would allow an optimistic view of its potential. The AASP is capable of responding to accelerations between 0.03 and 100 Hz. In the case of sustained accelerations, as in a slow turn maneuver, we take advantage of the fact that the velocity pickoff has a flat response to the rate of change of acceleration, $\dot{\gamma}$. This is the actual motion sensed. Under constant accelerations, then, the integrator must hold this value until another change in acceleration is sensed. The only error in the system output due to this maneuver is the integration error.

The resonance at 100 Hz is of no concern since it is well above the intended upper range of the instrument. Since this was attributed to an effect of the instrument dynamics and was excited by direct vibration of the isolation gimbal, there is some question whether it would even be present in an operational system where an extra gimbal is provided between the isolation gimbal and airframe. In any event, filtering of the output signal is suggested and aliasing would not be a problem at the actual frequencies at which the output would be sampled, say dc to 20 Hz.

Navigation

Although only the development of a single-axis vertical indicator was presented, the overall objective is to apply this to a navigation system. A three-axis navigation system may be configured with the use of two single-axis AASPs aligned on a single frame with orthogonal sensitive axes. An azimuth sensor, similar to the quartz fiber angular acceleration sensor in the AASP, is proposed for use on the yaw axis. This is equivalent to a "nontorquing" or "free-azimuth" system which has a fixed base, thus eliminating the torquing commands for the azimuth axis, but requiring an additional coordinate transformation in order to transfer from a local to a geocentric reference. Since the AASP is a vertical tracking system, the navigator takes advantage of the fact that perturbations of its vertical reference about the gravity axis will generally be of relatively short duration and is self-correcting in the sense that in the absence of linear accelerations (a constant cruise speed) the pendulum will seek the local vertical and thus track the rate of change of latitude and longitude.

It would be necessary to initially align the system with respect to a known external reference since self-alignment is not possible as in the case with gyroscopic systems. The two acceleration-sensitive axes should be aligned to the directions of lines of latitude and longitude. This could be accomplished with the use of a mirror on the outer transfer case. In actual development of a navigation system based on this device, it is suggested that a two-axis version of this system employing a spherical pendulum would be used.

No claim as to overall system navigation accuracy is made or implied. However, we feel that future development holds high promise for its potential. This is based simply on the accuracies found in the RAMP system utilizing this same concept⁴ and the fact that the remaining error source, the gyro, has been replaced with a "drift-free" angular accelerometer. The system proposed here, then, is nothing more than a refinement of the RAMP. The gyros were used in that system to measure the angular motion of the pendulum. We suggest that an angular differentiating accelerometer does it more simply and efficiently.

Acknowledgments

The development of the AASP was a team project and the authors gratefully acknowledge the assistance of D. R. Stevens and Bill Simmons from the F. J. Seiler Research Lab; Bill Whitesell, Craig Price, and Bob Thede from CIGTF, Holloman Air Force Base, and Art Throckmorton of Okubo Instruments, Inc.

References

- ¹Astrom, K. J. and Hector, N. F., "Vertical Indication with a Physical Pendulum Based on Electromechanical Synthesis of a High Moment of Inertia," TTN-Group Division of Applied Hydromechanics, Royal Institute of Technology, Stockholm, Sweden, Rept. 590802, Aug. 1959.
- ²Astrom, K. J., "A Schuler-tuned Three Gyro Platform System," TTN-Group, Division of Applied Hydromechanics, Royal Institute of Technology, Stockholm, Sweden, Rept. 591202, Dec. 1959.
- ³Hector, F., "The RAMP Inertial Navigation System," *Philips Technical Review*, Vol. 29, 1968, pp. 69-85.
- ⁴Koenke, E. J., "Analysis and Evaluation of a Novel Inertial Navigation System," NASA TRC-79, Cambridge, Mass., May 1969.
- ⁵Okubo, S., "Instrumentation for Precision Measurements," AIAA Paper 75-1080, Boston, Mass., Aug. 1975.